ANNALS OF BIOMEDICAL ENGINEERING 1, 160–181 (1972)

Mathematical Interrelationship Between Instantaneous Ventricular Pressure–Volume Ratio and Myocardial Force–Velocity Relation[1,2]

HIROYUKI SUGA AND KIICHI SAGAWA

Department of Biomedical Engineering,
The Johns Hopkins University, School of Medicine,
Baltimore, Maryland 21205

Received March 1, 1972

The instantaneous left intraventricular pressure–volume ratio, $e(t) = p(t)/[v(t) - v_d]$, in which $p(t)$, $v(t)$ and v_d are intraventricular pressure, volume and a correction factor, respectively, was shown by our experimental studies to be independent of mechanical loading conditions and yet vary markedly with changes in contractile state of the ventricle. The studies also indicated that the $e(t)$ curve under a given contractile state could be described as $e(t) = \alpha e_0(\beta t)$, in which $e_0(t)$ represents $e(t)$ under arbitrarily defined control contractile state and heart rate, and α and β are magnitude and duration parameters of the given $e(t)$ with respect to $e_0(t)$. The present mathematical analysis of mechanical relationship between ventricular performance represented by $e(t)$ and myocardial contraction shows that the α and β parameters related to myocardial force, F, and shortening velocity of contractile element, V_{ce}, respectively. Using a two-element model of myocardium and a thick-wall sphere or cylinder model of the ventricle we found that $F(t) = \alpha H e_0(\beta t)$ and $V_{ce}(t) = \beta K_j[de_0(\beta t)/d(\beta t)]/e_0(\beta t)$. Both H and K_j are functions of ventricular volume and are specific to the geometric model used, whereas the mode of afterload affects K_j only. The mathematically derived F–V_{ce} curves and their shifts owing to variations of α, β, H and K_j under isotonic, isobaric and isovolumetric contractions simulated the experimentally established F–V_{ce} curves from papillary muscle and their characteristic shifts reported by other investigators. On these bases we conclude that $e(t)$ explicitly expresses the dynamic characteristics of myocardial contractions, which further supports our experimental contention that $e(t)$ can be used as a useful index of contractile state of the ventricular chamber.

GLOSSARY OF SYMBOLS

$e(t)$	instantaneous left intraventricular pressure–volume ratio.
$e_0(t)$	$e(t)$ in an arbitrarily defined control contractile state and heart rate.
e_{max}	peak magnitude of $e(t)$.
t_{max}	time to e_{max} from the onset of systole.
α	magnitude parameter of $e(t)$.
β	time-duration parameter of $e(t)$.
$p(t)$	left intraventricular pressure.
$v_i(t)$	left intraventricular absolute volume.

[1] Abstract of this paper was presented in the fall meeting of the American Physiological Society (1971) [Suga, H. and Sagawa, K. *The Physiologist,* 1971, **14,** 239].

[2] Preliminary analysis was made by Hiroyuki Suga in Institute for Medical and Dental Engineering, Tokyo Medical and Dental University, Tokyo. Further analysis was supported in part of PHS Grant HE 14529.

v_m left ventricular wall volume (incompressible).
v_d volume correction factor.
v_{io} intraventricular unstressed volume when the left ventricle is not excited.
v_{ic} initial volume of the left ventricle given as preload.
$f_1(v_i)$ function only of $v_i(t)$ in a given ventricle, and parameter relating $e(t)$ to myocardial force.
$f_2(v_i)$ function only of $v_i(t)$ in a given ventricle, and length of a unit myocardial mass.
k elastic modulus of series elastic component in the unit myocardial mass.
$F(t)$ myocardial force generated by the unit myocardial mass.
$V_{ce}(t)$ shortening velocity of contractile element in the unit myocardial mass.
$H(v_{ic})$ function of v_{ic}, and parameter relating $e(t)$ to myocardial force.
$K_j(v_{ic})$ function of v_{ic}, and parameter relating $[de(t)/dt]/e(t)$ to shortening velocity of contractile element.

I. INTRODUCTION

The mechanical properties of the left ventricle as a pump are important for understanding overall circulatory dynamics. Ventricular contraction has been characterized at three arbitrary levels. The first is to regard the ventricle as a hydraulic element and define it in terms of its input–output relationships. Examples of such a characterization are Starling's law of the heart which relates cardiac output to mean atrial pressure (Patterson *et al.*, 1914) or the ventricular function curve which relates external mechanical work to enddiastolic pressure of the ventricle (Sarnoff *et al.*, 1962) and a cardiac output surface relating cardiac flow to arterial and venous pressures (Sagawa, 1967). The second level is to characterize it as an active chamber and describe ventricular contraction in terms of intraventricular pressure and volume variables. The examples are the pressure–volume diagram (Frank, 1895) and our pressure–volume ratio (Suga, 1969a, 1969b, 1970 and 1971a). The third level is to regard the ventricle as an assemblage of myocardial fibers and to describe their shortening characteristics in terms of the so-called force–velocity relation (Sonnenblick, 1962; Braunwald *et al.*, 1967).

Suga has shown experimentally that instantaneous left intraventricular pressure–volume ratio during systole uniquely characterizes the ventricular contractile state. A mathematical model of the heart based on the above findings simulated cardiac responses to various hemodynamic conditions (Suga, 1971b). This successful simulation suggests that the pressure–volume ratio serves as a bridge between the first and the second level of characterization of ventricular contraction discussed above.

The present purpose is to show that the time-varying pressure–volume ratio also relates the second level with the third level of characterization of ventricular contraction; we mathematically derive the known myocardial force–velocity relations from the left ventricular pressure–volume ratio curve. We use a series elastic and contractile element model of myocardium and either sphere or cylinder model of ventricular geometry for the derivation.

II. PHYSIOLOGICAL FINDINGS

Recently, Suga showed in the canine left ventricle that the course and magnitude of the time-varying ratio of instantaneous intraventricular pressure over absolute intraventricular volume was practically independent of preload and afterload imposed on the ventricle. As yet, the time course and magnitude of the ratio was found to vary sensitively to changes in the contractile state. We have reinvestigated these findings using a plethysmographic measurement of instantaneous left ventricular volume (see Appendix I for the method). The results of this experiment reconfirmed the earlier findings.[3] However, the study also indicated the necessity of redefining the ratio to insure its independency of mechanical loading conditions. Thus we defined the left ventricular pressure–volume ratio $e(t)$, using an experimentally obtained correction factor for ventricular volume:

$$e(t) \equiv p(t)/[v_i(t) - v_d], \tag{1}$$

in which $p(t)$ is left intraventricular pressure and $v_i(t)$ is left intraventricular absolute volume. v_d is the volume axis intercept of a straight line drawn throughout the left uppermost corners of a family of pressure–volume loops under a given contractile state at different pre- and afterloads as shown in Fig. 1. v_d was invariant with changes in contractile state or loading conditions (see Appendix II for further explanation of v_d).

[3] SUGA, SAGAWA AND SHOUKAS, Load-independency of instantaneous pressure–volume ratio of the canine left ventricle and effects of epinephrine and heart rate on the ratio, submitted for publication.

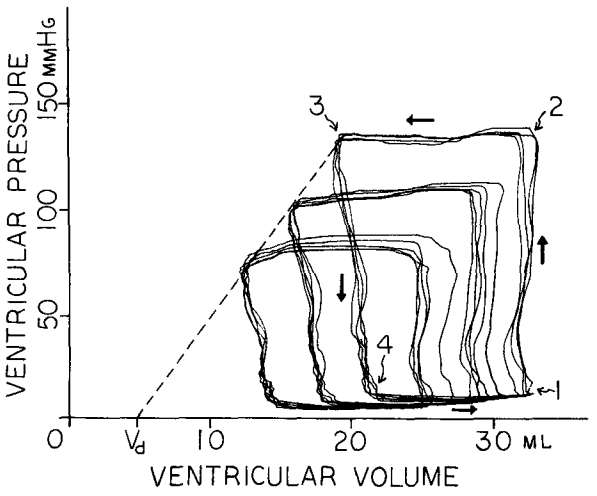

FIG. 1. Graphical explanation of correction volume v_d. v_d is the volume axis intercept of the broken straight line which is drawn to connect the left uppermost corners of a family of pressure–volume loops traced under a control contractile state and different ventricular loading conditions above and below normal preload and afterload. v_d was 4 ~ 6 ml for 20-kg dogs and remained constant even when the contractile state was altered by epinephrine infusion. The arrows show the direction of movement of a pressure–volume data point on the pressure–volume loop. Isovolumetric contraction phase (1–2), systolic ejection phase (2–3), isovolumetric relaxation phase (3–4) and diastolic filling phase (4–1).

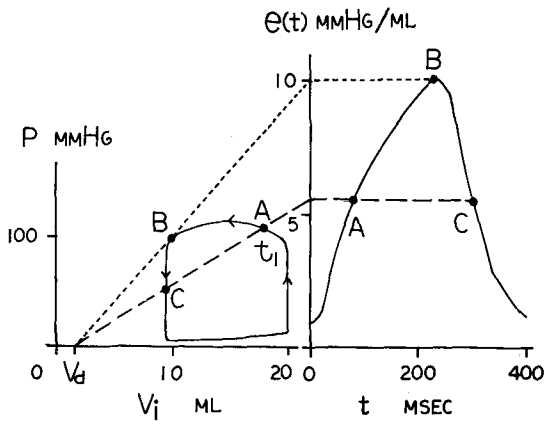

FIG. 2. Graphical explanation of $e(t)$. The left panel shows a pressure–volume loop in a contraction and the correction volume v_d. $e(t)$ is the slope of a line connecting a fixed point $(v_d,0)$ and another point $[v_i(t),p(t)]$. $e(t)$ is expressed by the height of the projection of this line on the appropriately scaled vertical line (e axis) in the center of the graph. As time goes on, the point $[v_i(t),p(t)]$ travels A, B and C on the pressure–volume loop changing the slope of the line and therefore the height of the projected point on the e axis. The right panel shows the time course of the slope of the line in the left panel, points A, B and C in the right panel corresponding to those in the left panel.

Figure 2 is a schematic illustration of our new definition of $e(t)$ on a pressure–volume plane. Given a time point (t_1) during systole, the pressure–volume ratio $e(t_1)$ is represented by the slope of a line which connects a fixed point (v_d,o) and another point $[v_i(t_1), p(t_1)]$ on the pressure–volume loop indicating a cardiac cycle. This latter point moves with time from A to B and C, changing the slope of the line which represents $e(t)$. The time-varying slope of the line is plotted as an explicit function of time in the right side of Fig. 2.

Shown in Fig. 3A is the experimental recording of $e(t)$ curve (channel 3) calculated by an electronic divider from the intraventricular pressure and volume tracings in channels 1 and 2. When cardiac output was altered by changing preload, intraventricular pressure changed as is shown in the first channel. However, the peak value of $e(t)$, e_{max}, and time to e_{max} from the onset of systole, t_{max}, were not affected ($P > 0.5$) by these changes in preload and afterload.

Shown in Fig. 3B is the recording obtained when cardiac output increased while peak intraventricular pressure was maintained constant. The third channel shows that e_{max} and t_{max} were not affected by the change in preload. The load-independency of e_{max} and t_{max} was also observed when arterial pressure was varied while maintaining cardiac output constant.

Figure 3C shows that e_{max} was markedly increased ($P < 0.001$) and t_{max} was shortened ($P < 0.001$) with increases of epinephrine infusion from 0 to 1 and 2μg/kg/min. We also noted similar load-independency of e_{max} and t_{max} values under the enchanced contractile state. Figure 3D shows the effect of heart rate on e_{max} and t_{max}. t_{max} shortened with graded increases in heart rate, controlled by ventricular pacing, whereas e_{max} did not change. From nine experimental preparations the mean e_{max} value was 6.6 ± 1.2 (SD) mmHg/ml and the mean t_{max} value

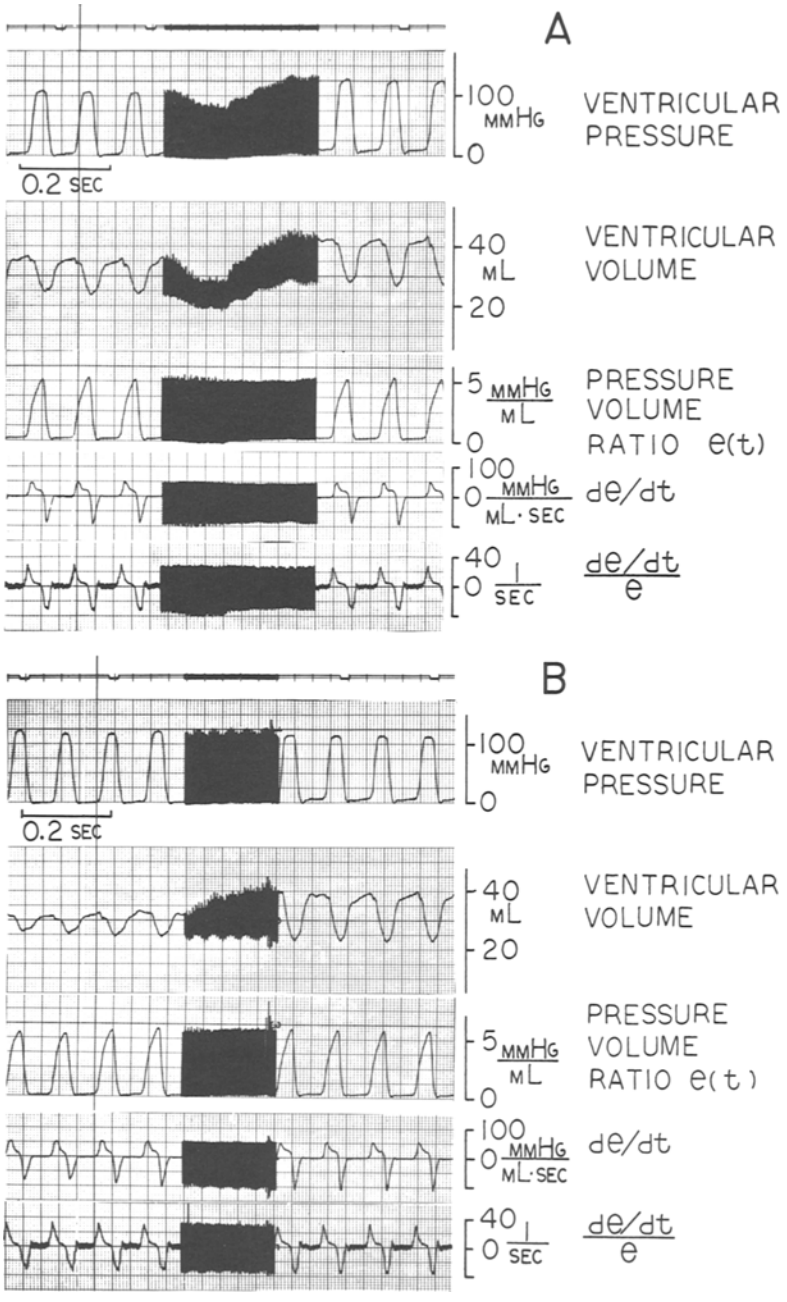

FIG. 3. The instantaneous pressure–volume ratio curves of a canine left ventricle. The $e(t)$ curves in the third channel are computed from the intraventricular pressure (first channel) and volume (second channel). Panels A and B show the data when cardiac output was varied with and without secondary changes in mean arterial pressure, respectively. Panel C shows the relationship of $e(t)$ curves with different rates of epinephrine infusion. Panel D are the data while heart rate was varied by electrical pacing of the ventricle. In channels 4 and 5 of all the panels are the time-derivatives of $e(t)$ and $(de/dt)/e$, respectively. de/dt was computed by a CR network with a time constant of 0.5 msec and $(de/dt)/e$ was computed by an analog computer.

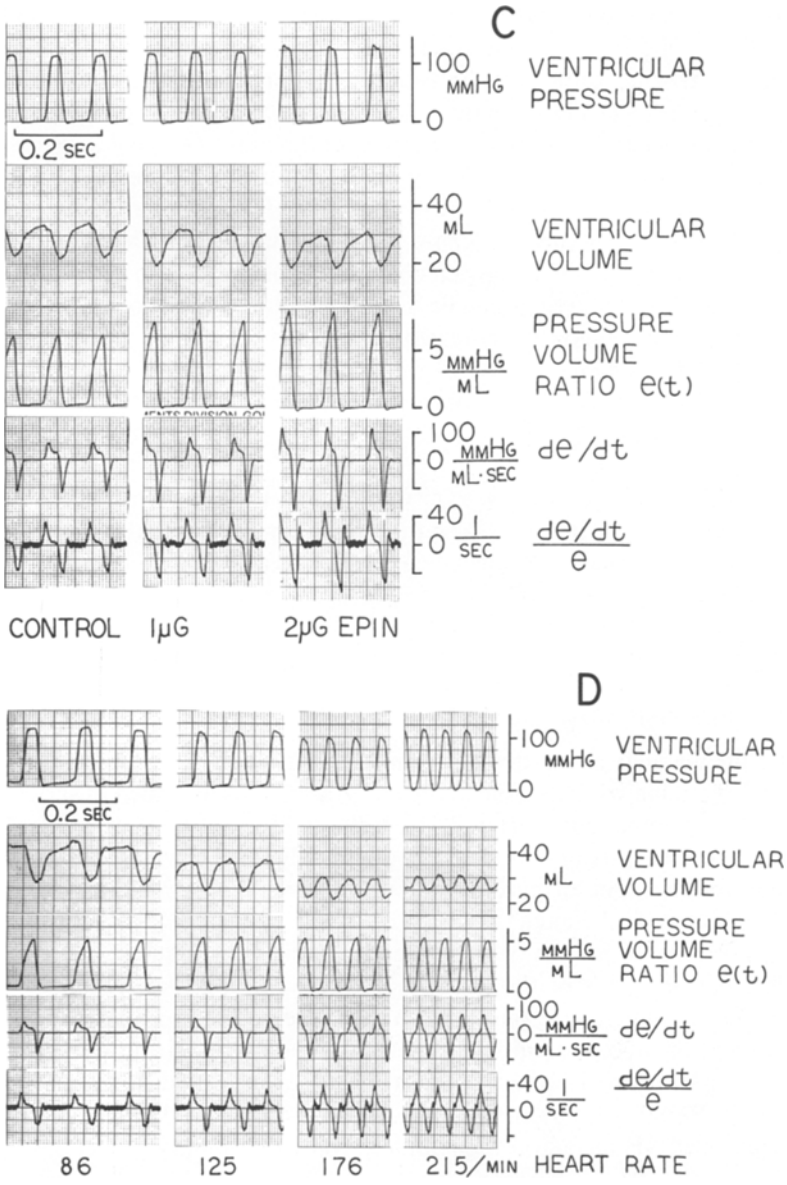

FIG. 3. *Continued.*

was 191 ± 29 msec before epinephrine infusion and 12.2 ± 4.5 mmHg/ml and 157 ± 26 msec during 2μg/kg/min epinephrine infusion, respectively.

The similitude of the shape of $e(t)$ curves was checked statistically after normalizing all the experimental $e(t)$ curves by making both e_{max} and t_{max} values unity. From this result we conclude that all $e(t)$ curves have a unique shape regardless of different e_{max} and t_{max} values. Therefore, e_{max} and t_{max} are considered as the characteristic parameters of $e(t)$ curves.

Based on the above findings, we introduced two parameters α and β. α is the ratio of e_{max} under a given contractile state over that under an arbitrarily defined control contractile state. β is the ratio of t_{max} under the control contractile state over that under the given contractile state. Both α and β parameters are unity under a control contractile state, and greater than unity when e_{max} is increased and t_{max} is shortened in the case of enhanced contractile state. α was found to be 1.8 ± 0.6 (SD) and β was 1.3 ± 0.1 during $2\mu g/kg/min$ epinephrine infusion. As mentioned before, α did not change during increases in heart rate whereas β increased at the rate of 45% per change in 100 beats/min. α and β, which are parameters of e_{max} and t_{max}, can be used as empirical measures of a change in contractile state from a control contractile state.

Because of the similitude of all the observed $e(t)$ curves, we can mathematically express $e(t)$ under any contractile state as

$$e(t) = \alpha e_0(\beta t), \tag{2}$$

in which $e_0(t)$ is a particular $e(t)$ determined under arbitrarily defined control contractile state and heart rate. In the present mathematical analysis, we assume that Eq. (2) is also valid for special cases such as afterloaded isotonic, isobaric and isovolumetric contractions.

III. MATHEMATICAL ANALYSIS

A. Two-Element Model of the Myocardial Fiber

The mechanical properties of the myocardial fiber are represented by a three-element model in which a contractile element (CE) is arranged in series with a passive elastic component (SE) and in parallel with another passive elastic element (PE). In the analysis of contractile process, PE is usually neglected for simplicity considering that it contributes minimally to force development (Braunwald *et al.*, 1967; Donders and Beneken, 1971).

The property of SE has been studied by the so-called quick release method and is described in terms of the relationship between a passive change in its length (Δl_s) and the change in applied force (ΔF). We will be considering in this analysis a unit mass of myocardium which has unit length (1 cm) and unit cross sectional area (1 cm^2) when the muscle mass is not excited and completely unstressed ($F = 0$).[4] Parmley and Sonnenblick (1966) reported the following empirical description of SE based on their findings on cat papillary muscle:

$$dl_s/dF = (k \cdot F + C)^{-1},$$

in which l_s is the length of SE in the unit mass, F the applied force and C a constant. k represents the elastic modulus of SE and is believed to be unaffected by

[4] In the present study the definition of a unit mass of myocardium is the myocardium mass of unit volume (1 cm^3) whose length and cross sectional area are unity (1 cm and 1 cm^2) when the muscle is not excited and no preload is applied to it. This definition is convenient when we compare the mathematical data with experimental data. In papillary muscle experiments elastic modulus of SE, myocardial force and shortening velocity of CE are conventionally normalized for the dimensions of the muscle mass at a particular condition and not for the instantaneous dimensions.

contractile process nor by a change in contractile state of myocardium. The value of the constant C is small compared with the value of $k \cdot F$ over the physiological range of F. Therefore, the above equation can be approximated by

$$dl_s/dF = (k \cdot F)^{-1}. \tag{3}$$

On the basis of experimental findings on papillary muscle (Sonnenblick, 1962) the shortening property of CE has been described in terms of the relationship between the force actively developed by CE and its shortening velocity. Given an appropriate model of ventricular geometry and the relationship between the ventricular wall stress and lumen pressure, one should be able to derive a similar force–velocity relation from ventricular pressure–volume relation. This has been done in various manners (Sandler and Dodge, 1963; Fry *et al.*, 1964; Levine and Britman, 1964; Ross *et al.*, 1966, and McDonald *et al.*, 1966). We use here a new way to translate ventricular pressure and volume variables into force and shortening velocity of muscle, in which the time course of ventricular pressure–volume ratio, $e(t)$, is fully utilized.

B. Geometric Models of the Left Ventricle

Relationships between myocardial force and left intraventricular pressure and between myocardial length and left intraventricular volume would be precisely determined if we have detailed knowledge of morphology of the left ventricle. This work is still under an extensive investigation by other investigators (Mirsky, 1969; Armour and Randall, 1970).

To simplify the analysis we use either a thick-wall sphere or a thick-wall cylinder model with the following assumptions: (1) Left ventricle has an identical shape throughout a cardiac cycle, (2) Distribution of myocardial fibers in the ventricular wall is isotropic and homogeneous in the sphere model while it is circular in the cylinder model, (3) All the fibers contract simultaneously, and (4) Left intraventricular pressure is in instantaneous equilibrium with myocardial force. Both these geometric models and assumptions have been used in the above-mentioned earlier analysis of left ventricular mechanics.

1. Thick-wall sphere model. We assume that the left ventricle be a thick-wall hollow sphere with the inside radius R_i, outside radius R_o, intraventricular volume v_i, and wall volume v_m which is incompressible through the cardiac cycle. If we consider that the average circumferential force F is generated in the unit mass at the equator, then the force thus normalized is related to the radii and the transmural pressure as

$$F(t) = p(t)R_i(t)^2/(R_{oo}^2 - R_{io}^2), \tag{4}$$

in which R_{oo} and R_{io} are the R_o and R_i when the ventricle is not excited and the transmural pressure is zero, namely $p = 0$ and $F = 0$ (see Footnote 5). Moreover,

[5] The total circumferential force is given by $\pi R_i(t)^2 p(t)$. When the total force is normalized for the cross sectional area of the above defined unit mass, we obtain Eq. 4. If the total force is normalized for instantaneous unit cross sectional area it gives "stress" and is equal to

$$p(t)R_i(t)^2/[R_0(t)^2 - R_i(t)^2].$$

$$v_i(t) = (4/3)\pi R_i(t)^3,$$
$$v_m = (4/3)\pi[R_o(t)^3 - R_i(t)^3],$$

and the unstressed intraventricular volume v_{io} when the ventricle is not excited and $p = 0$ is

$$v_{io} = (4/3)\pi R_{io}^3.$$

Using $e(t)$ defined by Eq. (1), Eq. (4) can be rewritten as

$$F(t) = e(t) \cdot v_i(t)^{2/3}[v_i(t) - v_d]/[(v_{io} + v_m)^{2/3} - v_{io}^{2/3}]. \quad (5)$$

We consider that the length of the above-mentioned unit myocardium mass at the average radius, $0.5(R_i + R_0)$, is the representative fiber length supporting the average force F. This fiber length is then the sum of length l_c of CE and length l_s of SE. Therefore,

$$l_c(t) = \{[v_i(t) + v_m]^{1/3} + v_i(t)^{1/3}\}/[(v_{io} + v_m)^{1/3} + v_{io}^{1/3}] - l_s(t). \quad (6)$$

2. Thick-wall cylinder model. Alternatively, we will assume the left ventricle to be a thick-wall cylinder with constant height and constant wall volume v_m, neglecting muscle volumes of the top and bottom walls. The average circumferential force F generated by the unit myocardium mass and the length of CE in the same unit mass are given by

$$F(t) = e(t) \cdot v_i(t)^{1/2}[v_i(t) - v_d]/[(v_{io} + v_m)^{1/2} - v_{io}^{1/2}] \quad (7)$$

and

$$l_c(t) = \{[v_i(t) + v_m]^{1/2} + v_i(t)^{1/2}\}/[(v_{io} + v_m)^{1/2} + v_{io}^{1/2}] - l_s(t). \quad (8)$$

C. General Formulations of Myocardial Force and Length of CE

Equations (5)–(8) lead to the two general equations for the normalized myocardial force and length of CE with respect to the unit myocardium mass:

$$F(t) = f_1[v_i(t)]e(t), \quad (9)$$

$$l_c(t) = f_2[v_i(t)] - l_s(t). \quad (10)$$

f_1 and f_2 are mathematical functions only of $v_i(t)$, with parametric constants v_m, v_{io} and v_d. These three parameters can be specified for a given ventricle; therefore, f_1 and f_2 values are determined only through the resultant intraventricular volume. The forms of the f_1 and f_2 functions are shown in Eqs. (5)–(8) and are specific to the type of the geometric model used.

Equation (9) shows that the normalized force F is related to the intraventricular volume by $e(t)$. Since our experiments indicate that $e(t)$ remains the same regardless of mode of afterload, the relationship between F and v_i is independent of the mode of afterload. A similar independence in the force–length relationship from afterload was shown to exist in cat papillary muscle by Downing and Sonnenblick (1964). These investigators contracted the muscle from various initial fiber lengths under different modes of afterload, including isotonic, isometric and afterload istonic contractions. In Fig. 4A, which was reproduced from their paper, the endsystolic points determined from these different contractions were plotted

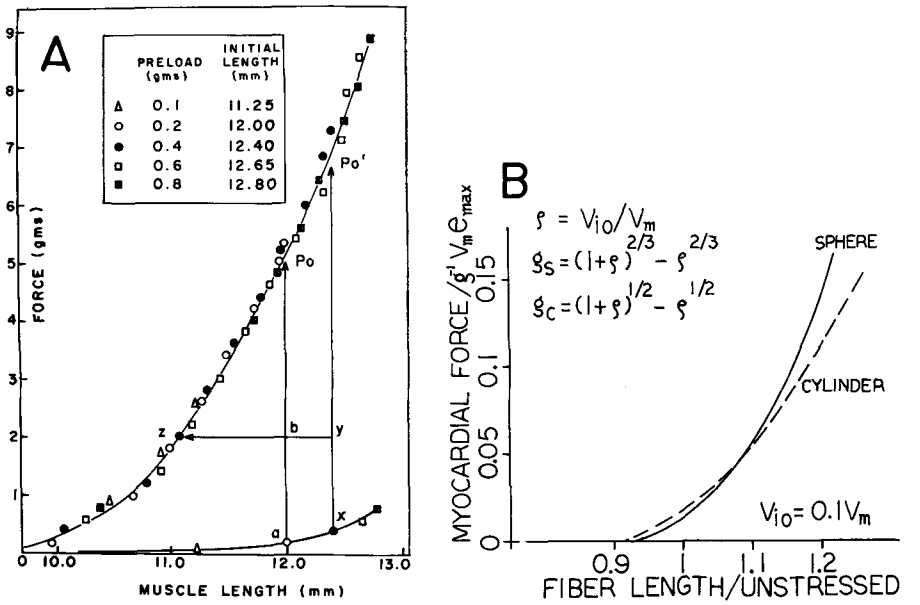

FIG. 4. Comparison of experimental and mathematical force–length relationship curves.

(A) Force–length relationship curve of a cat papillary muscle [Reproduced from Fig. 1B of Downing and Sonnenblick (1964) with the permission of the author and publisher]. Muscle length with 0.2-g preload is 1.2 cm, cross sectional area 0.011 cm^2, stimulation frequency = 12/min, temperature = 22°C. P_o = total force developed from an initial length a when the afterload was of such a magnitude that muscle shortening did not occur; p_o' similar to p_o but from different initial length x. Note that the muscle shortened to the same point on the active length force curve (z) independent of its initial length as far as the afterload was constant. Thus the plot indicates that isometric and isotonic force–length curves are virtually identical. When force value is normalized with respect to 1-cm^2 cross sectional area of myocardium, 1g/0.011 cm^2 = 90 g/cm^2.

(B) Mathematical relation between maximum total force and length of the unit myocardial mass which has unit length and cross sectional area when it is not excited and unstressed. Two sets of data were calculated for both the thick-wall sphere and cylinder models of ventricular geometry. The ordinate is myocardial force normalized with respect to $g^{-1}v_m e_{max}$, in which g (g_s for the sphere, g_c for the cylinder model) stands for the equation in this panel. The abscissa is fiber length normalized with respect to its unstressed length. For example, myocardial force value 0.1 is equal to 95 g/cm^2 for the sphere model and 110 g/cm^2 for the cylinder model when v_m = 100 ml, v_{io} = 0.1 v_m, v_d = 5 ml and e_{max} = 6 mmHg/ml as representative values in a 20-kg dog.

on a force–length plane and these points gathered around a single curve regardless of the afterload conditions. We compared this experimental curve in Fig. 4A with the mathematically derived curve from Eqs. (9) and (10) which is shown in Fig. 4B. The similarity of these two curves suggests that the load-independency of $e(t)$ is a valid concept of ventricular contractile process.

D. General Formulations of Shortening Velocity of CE

Shortening velocity V_{ce} of CE is given by the negative time-derivative of length of CE: $V_{ce}(t) = -dl_c/dt$. The time-derivative of Eq. (10) yields

$$-dl_c/dt = -d\{f_2[v_i(t)]\}/dt + dl_s(t)/dt.$$

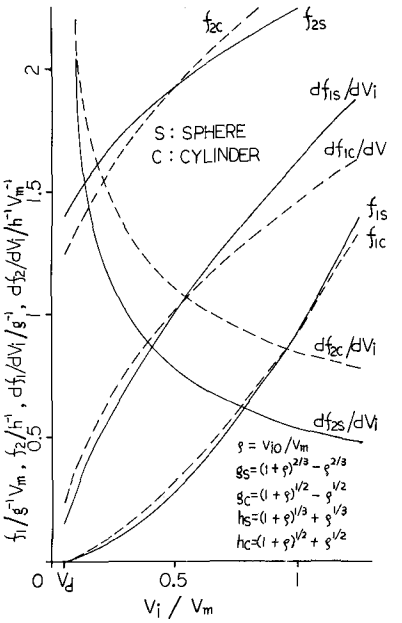

FIG. 5. Graphical presentation of f_1, f_2 and their derivatives as a function of v_i in the thick-wall (——) and cylinder (– – –) models. $f_1/g^{-1}v_m$ means that f_1 is normalized with respect to $g^{-1}v_m$, and the same holds for f_2, df_1/dv_i, df_2/dv_i. Subscripts s and c denote the sphere and cylinder models, respectively. Mathematical functions g's and h's represent denominators normalized with respect to v_m in the mathematical formulas of f_1, f_2 and their derivatives. v_d, v_m and v_{io} have the same values as in the explanation to Fig. 4B.

Since f_2 is a function only of $v_i(t)$ in a given ventricle the first term of the above equation can be rewritten as $-(df_2/dv_i) \cdot [dv_i(t)/dt]$. The second term can also be rewritten as $(dl_s/dF) \cdot (dF/dt)$. Accordingly,

$$V_{ce} = -[df_2(v_i)/dv_i] \cdot [dv_i(t)/dt] + [dl_s/dF] \cdot [dF(t)/dt]. \quad (11)$$

Substitution of Eqs. (3) and (9) and $df_1/dt = (df_1/dv_i)(dv_i/dt)$ into Eq. (11) gives

$$V_{ce}(t) = -[dv_i(t)/dt][df_2/dv_i - (df_1/dv_i)/(kf_1)] + [de(t)/dt]/[ke(t)]. \quad (12)$$

k is the elastic modulus of SE used in Eq. (3). f_1, f_2 and their derivatives with respect to v_i are specific to each of the two geometric models (see Appendix III). The graphical relationships of f_1 and f_2 versus v_i values are shown for the sphere and cylinder models in Fig. 5. It indicates that they bear similar relationships to v_i both qualitatively and quantitatively.

E. Force–Velocity Curve Derived from e(t)

Elimination of the time variable from Eqs. (9) and (12) results in force (F)–velocity (V_{ce}) relation of CE. The parameters of force–velocity relation, $v_i(t)$ and $dv_i(t)/dt$, depend on the mode of ventricular afterload. Three representative modes of afterload will be used for the analysis.

1. Afterloaded isotonic contraction. Afterloaded isotonic contraction is de-

fined when $F(t)$ is kept at a specified constant level throughout the ejection phase. Therefore, $dF(t) = 0$ during the ejection phase. From the time-derivative of Eq. (9),

$$dF(t)/dt = [df_1(v_i)/dv_i][dv_i(t)/dt]e(t) + f_1[v_i(t)][de(t)/dt] = 0.$$

Rearranging,

$$-dv_i(t)/dt = \{f_1[v_i(t)]/[df_1(v_i)/dv_i]\} \cdot [de(t)/dt]/e(t). \tag{13}$$

Substituting Eq. (13) into Eq. (12) yields

$$V_{ce}(t) = \{f_1[v_i(t)] \cdot [df_2(v_i)/dv_i]/[df_1(v_i)/dv_i]\} \cdot [de(t)/dt]/e(t).$$

Denoting the quantity within the braces by K_1,

$$V_{ce}(t) = K_1 \cdot [de(t)/dt]e(t). \tag{14}$$

Note that K_1 is a function only of the instantaneous left ventricular volume, $v_i(t)$, in a given ventricle.

2. *Afterloaded isobaric contraction.* Afterloaded isobaric contraction is defined as a contraction when $p(t)$ is kept constant through the ejection phase. Therefore, $dp(t)/dt = 0$ during the ejection phase. Accordingly, from Eq. (1),

$$dp(t)/dt = [v_i(t) - v_d]de(t)/dt + e(t)dv_i(t)/dt = 0.$$

Rearranging,

$$-dv_i(t)/dt = [v_i(t) - v_d] \cdot [de(t)/dt]/e(t). \tag{15}$$

Substituting Eq. (15) into Eq. (12), we obtain

$$V_{ce}(t) = \{[v_i(t) - v_d]df_2(v_i)/dv_i + [1 - (v_i(t) - v_d) \cdot (df_1/dv_i)/f_1(v_i)]/k\} \times [de(t)/dt]/e(t).$$

Substituting K_2 for the content of the braces in the above equation, we obtain

$$V_{ce}(t) = K_2 \cdot [de(t)/dt]/e(t). \tag{16}$$

K_2 is a function only of the instantaneous left ventricular volume $v_i(t)$ in a given ventricle.

3. *Isovolumetric contraction.* Isovolumetric contraction means that $v_i(t)$ remains constant throughout a cardiac cycle or $dv_i\ (t)/dt = 0$ at any time in systole. Substituting this into Eq. (12), we obtain

$$V_{ce}(t) = (1/k)[de(t)/dt]/e(t).$$

Substituting K_3 for k^{-1}, we obtain

$$V_{ce}(t) = K_3 \cdot [de(t)/dt]/e(t). \tag{17}$$

4. *Generalized formulation.* From Eqs. (14), (16), and (17) which describe V_{ce} as a function of $[de(t)/dt]/e(t)$ for the three modes of ventricular afterload in this analysis we can obtain a generalized equation for V_{ce} on $e(t)$:

$$V_{ce}(t) = K_j \cdot [de(t)/dt]/e(t). \tag{18}$$

This equation means that V_{ce} at any instant of time during systole is obtained from the product of $[de(t)/dt]/e(t)$ and K_j which represents the mode of contraction and type of model used.

Conventionally the relation between afterload force and shortening velocity of CE of myocardium is defined by multiple sets of force and initial velocity values of isotonic contractions at specified initial fiber lengths (Sonnenblick, 1962; Braunwald *et al.*, 1967). Similarly we can assign a fixed value v_{ic} to the initial volume of our left ventricular model which specifies the initial length of the unit myocardial mass. We can then compute the shortening velocities of CE at the onset of ejections against a variety of afterload to be developed and maintained throughout the ejection period in case of afterloaded isotonic or isobaric contraction. In case of isovolumetric contraction, the initial fiber length is maintained throughout cardiac cycle while the fiber develops force. Under these circumstances, K_j, which represents the mode of afterload, is a function of the given initial ventricular volume, v_{ic}.

From Eq. (9), a generalized form of F can be written as

$$F(t) = H \cdot e(t), \tag{19}$$

where H is equal to $f_1(v_{ic})$. H is independent of the mode of ventricular afterload, but is specific to a particular ventricular model.

It should be remembered here that both K_j and H are functions of the initial ventricular volume v_{ic} or preload in a given ventricular model. The relation of K_j and H versus v_{ic} are shown in Fig. 6 for both the sphere and cylinder models.

The force-velocity curve can be determined by plotting $F(t) = H \cdot e(t)$ against $V_{ce}(t) = K_j[de(t)/dt]/e(t)$, where H and K_j are constant if v_{ic} is speci-

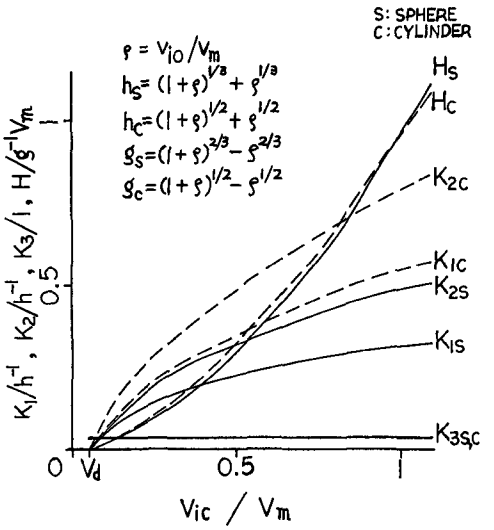

FIG. 6. Graphical presentation of K_1, K_2, K_3 and H as a function of initial ventricular volume v_{ic} in the thick-wall sphere (——) and cylinder (– – –) models. K_1/h^{-1} means that K_1 is normalized with h^{-1}. The same holds for K_2, K_3, H and v_i. K_3 is the reciprocal of the series elastic modulus k and common to both sphere and cylinder models.

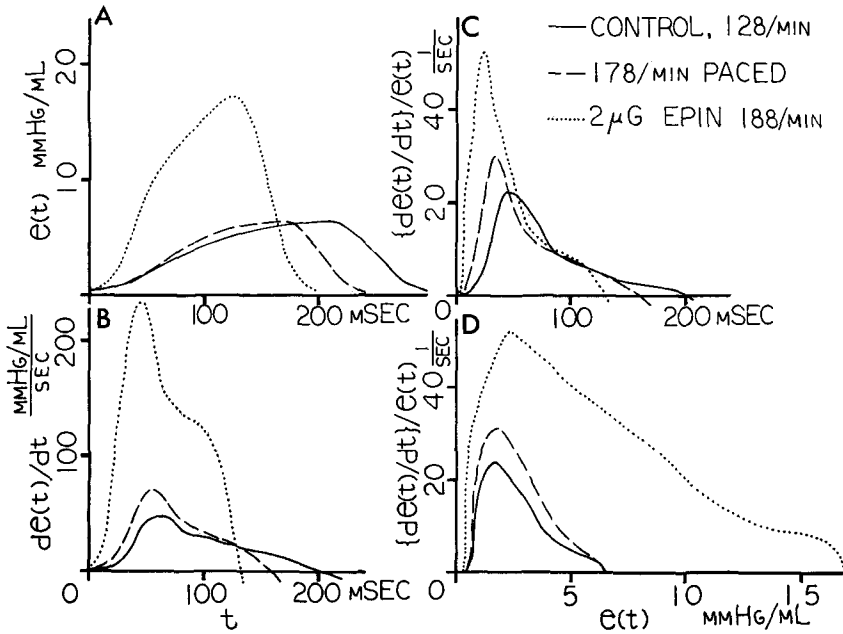

FIG. 7. Experimentally obtained $e(t)$ curves (A), $de(t)/dt$ curves (B) and $[de(t)/dt]/e(t)$ curves (C) plotted against time and $[de(t)/dt]/e(t)$ versus $e(t)$ curves (D) under control contractile state (——), during increased heart rate (– – –) and under an enhanced contractile state by epinephrine infusion of 2μg/kg/min (• • •) in a 20-kg dog.

fied. The fundamental characteristic shape of the force–velocity curve is solely determined by $e(t)$ on the abscissa versus $[de(t)/dt]/e(t)$ on the ordinate. Stretching this curve H times along the abscissa and K_j times along the ordinate gives the force–velocity curve. Shown in bottom channel of Figs. 3A, B, C and D are the $[de(t)/dt]/e(t)$ curves computed from $e(t)$ and $de(t)/dt$ curves in the third and fourth channels. $[de(t)/dt]/e(t)$ was not affected by changes in loading conditions (Panels A and B). However, increasing the rate of epinephrine infusion or increasing heart rate augmented the peak values of $[de(t)/dt]/e(t)$ as shown in Panels C and D. Figure 7 shows the experimentally obtained $e(t)$ versus $[de(t)/dt]/e(t)$ curves in Panel D, calculated from the data in Panels A, B and C under a control contractile state and heart rate (solid line). Superimposed are the $e(t)$ versus $[de(t)/dt]/e(t)$ curves under increased heart rate by pacing (dashed line) and enhanced contractile state by epinephrine infusion (dotted line). These three $e(t)$ versus $[de(t)/dt]/e(t)$ curves are similar in shape to each other. A family of myocardial force–velocity curves are calculated for the sphere model by multiplying the ordinate and abscissa of the experimentally obtained $e(t)$ versus $[de(t)/dt]/e(t)$ curve by K_j (v_{ic}) and $H(v_{ic})$, respectively, as shown in Fig. 8. The force–velocity curve calculated for the sphere model is similar to that for the cylinder model.

As given by Eq. (2), any $e(t)$ curve could be normalized with respect to a control $e(t)$, $e_0(t)$, in terms of two parameters α and β. We can analyze how the α and

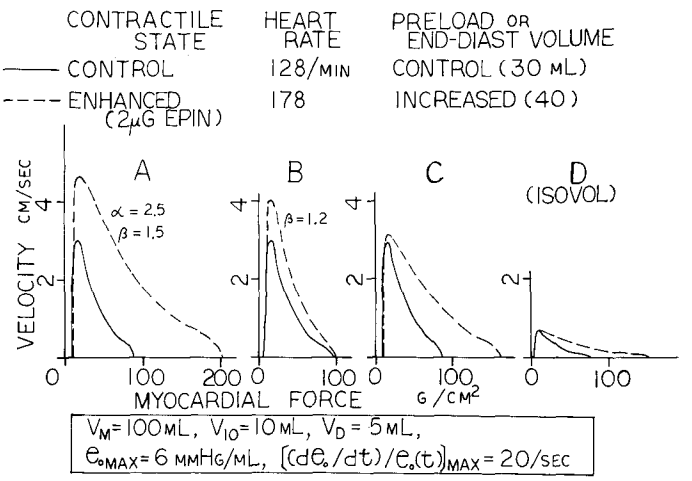

FIG. 8. Mathematical force–velocity curves derived from experimentally obtained $e(t)$ and $[de(t)/dt]/e(t)$ under changes in contractile state (A), heart rate (B) and preload (C and D). Force and velocity values are normalized with respect to the unit myocardial mass. The thick-wall sphere model is used; $v_m = 100$ ml, $v_{io} = 10$ ml, $v_d = 5$ ml, e_{max} for $e(t)$ under control contractile state is 6 mmHg/ml, and the peak value for $[de(t)/dt]e(t)$ under the control contractile state is 20/sec. These values are representative for a 20-kg dog. The force–velocity curves in Panels A, B and C are computed for isotonic contractions at a control initial volume of 30 ml. The curves for isobaric contraction and those computed with the thick-wall cylinder model do not greatly differ from these curves illustrated here. In case of isovolumetric contraction (D) the force value is completely independent of the preload, and determined only by the series elastic modulus. $\alpha = 2.5$ and $\beta = 1.5$ in an enhanced contractile state by 2μg/min/kg epinephrine infusion whereas $\alpha = 1$ and $\beta = 1.2$ during increased heart rate from 128 to 178/min. An increase of preload volume from 30 ml to 40 ml almost doubles H, whereas it increases K_1 and K_2 only to 1.2 times. K_3 does not change with the increase in preload volume.

β parameters affect the myocardial force–velocity relation. Differentiating Eq. (2),

$$de(t)/dt = \alpha \cdot \beta \cdot de_0(\beta t)/d(\beta t). \tag{20}$$

Substituting Eqs. (2) and (20) into (18) and (19), we obtain

$$V_{ce}(t) = \beta \cdot K_j \cdot [de_o(\beta t)/d(\beta t)]/e_o(\beta t) \tag{21}$$

and

$$F(t) = \alpha \cdot H \cdot e_o(\beta t). \tag{22}$$

The implications of Eqs. (21) and (22) are that when the α parameter is changed by some amount the force–velocity relation is only altered by an equal amount along the force axis. Similarly changes in the β parameter alters the force–velocity relation only along the velocity axis. These changes in the α and β parameters are also illustrated graphically in Fig. 8. On these bases, we can conclude that α is directly related to the relative magnitude of the maximum isometric force parameter (customarily denoted by P_o) and β represents the relative magnitude of the actually measured maximum shortening velocity (often called "measured" V_{max}). The α and β parameters are measures of the changes of the force–velocity relation and therefore the contractile state of the left ventricle.

IV. COMPARISON WITH PHYSIOLOGICAL DATA

A. Form of The Force-Velocity Curve Derived From e(t)

As seen in Fig. 8, the basic form of the force-velocity curve derived from $e(t)$ indicates an inverse curvilinear relation between $e(t)$ on the force axis and $[de(t)/dt]/e(t)$ on the velocity axis, independent of the type of geometric model and mode of contraction. The shape of the mathematically obtained curve resembles those obtained on mammalian papillary muscle contracting isotonically (Sonnenblick, 1962; Braunwald *et al.*, 1967). The calculated curve near the force axis intercept sharply curves downward. This is also true with the experimental curves from papillary muscle (Brutsaert and Sonnenblick, 1969). This had been considered to be due to the lack of sustained active state near the peak of force development. But Brutsaert and Sonnenblick (1969) showed the possibility that it depends rather on the presence of series elastic component that reduces the length of contractile element at higher loads. The early systolic portion of the calculated force-velocity curve is different from a hyperbolic curve. This deviation exists in experimentally obtained force-velocity curves and is considered to result from the delay for active state to reach its maximum (Sonnenblick, 1965).

B. Effects of Contractile State

Our experimental studies showed that both α and β were markedly increased under enhanced contractile state by stellate ganglion stimulation or epinephrine infusion and both decreased when contractile state was depressed by pentobarbital or acetylcholine infusion (Suga, 1969a, 1969b, 1970 and 1971a; Suga *et al.*, 1971). Figure 8A shows that the mathematically derived force-velocity curves shifted with changes in contractile state. The force value is increased α times and the velocity value increased β times. It is known that the force-velocity curve

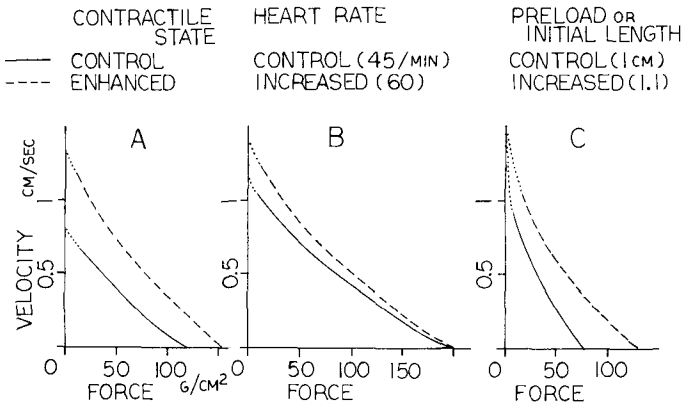

FIG. 9. Typical force-velocity curves experimentally determined on cat papillary muscle contracting isotonically and their characteristic shifts associated with an increase in contractile state by epinephrine (A), stimulation rate (B) and preload or initial length (C) [Reproduced from Figs. 6A, 10A1 and 10A2 of Sonnenblick (1962) with the permission of the author and publisher]. Force and velocity values are normalized with respect to unit myocardial mass with unit dimensions (1×1 cm^2) when it is not excited and stretched by small preload.

obtained from mammalian papillary muscle shifts to the right and upward under enhanced contractile state as shown in Fig. 9A, and under a depressed contractile state left and downward (Sonnenblick, 1962). The effects of changes in contractile state on the force–velocity curve derived from $e(t)$ curves are consistent with those found on the directly measured physiological curve. These consistencies support our contention that $e(t)$ can be used as a comprehensive expression of the contractile state of the ventricle on the ventricular chamber level.

C. *Effects of Heart Rate*

Our experimental data indicated that the value of α remained constant over a wide range of heart rate (50 ~ 220/min) while β was significantly increased by increases in heart rate. The effects of alterations in heart rate on the force–velocity relations is to multiply the velocity value β times, leaving the force value unchanged as shown in Fig. 8B. Experimentally determined force–velocity curves of mammalian papillary muscle are shown in Fig. 9B which exhibits similar shifts [Sonnenblick (1962), Braunwald *et al.* (1967) and Kavaler *et al.* (1971)].

D. *Effects of Preload Ventricular Volume*

The α and β parameters are independent of changes in left ventricular end-diastolic volume as long as a contractile state remains constant. However, changes in preload intraventricular volume alter H and K_j parameters. H is approximately proportional to $v_{ic}^{5/3}$ in the sphere model and $v_{ic}^{3/2}$ in the cylinder model. K_j in the isotonic and isobaric contractions is approximately proportional to $v_{ic}^{1/3}$ in the sphere model and $v_{ic}^{1/2}$ in the cylinder model. Therefore a change in H caused by a change in v_{ic} is about three times for the cylinder model and five times for the sphere model larger than that of K_j in the isotonic and isobaric contractions. K_3, for isovolumetric contraction, is unaffected by changes in v_{ic} and is constant since the series elastic modulus k is constant. Figures 8C and D show the mathematically obtained shifts of the force–velocity curve by changes in preload ventricular volume v_{ic} in an isotonic contraction and an isovolumetric contraction, respectively. The experimentally obtained force–velocity curves indicated a remarkable change in force associated with alteration in preload, with a minimal difference in the extrapolated V_{max} value as is shown in Fig. 9C (Sonnenblick, 1962). However, Parmley *et al.* (1972) reevaluated the relationship of V_{max} and preload in higher ranges of initial muscle length. They showed that the extrapolated V_{max} using the two-element myocardial model slightly increased with increases in preload in isotonic contractions. In isometric contractions V_{max} was independent of preload. These findings are in agreement with our mathematical calculations. However, they noticed that, when preload approached a level at which the muscle developed maximum force, V_{max} tended to decrease with increases in preload. This finding is not consistent with our mathematical analysis.

E. *Effects of Mode of Contraction*

The mathematical analysis indicates that V_{ce} will be different for given F and v_{ic} in different modes of contraction. As shown in Fig. 6, K_3 for isovolumetric contraction is smaller than K_1 for the isotonic contraction and K_2 for the isobaric con-

traction in the sphere and cylinder models. Figure 8D is the force–velocity curve in isovolumetric contraction, in which V_{ce} was significantly smaller for given F and v_{ic} than in isotonic contraction (Panel C). Parmley *et al.* (1970) noticed that V_{ce} was smaller in isometric contraction as compared to isotonic contraction for the same force. This is consistent without analysis.

V. DISCUSSION

There are two ways of mathematically analyzing the correspondence between ventricular pressure–volume relationship and myocardial force–velocity relation. The first way is to reduce pressure–volume relationship to force–velocity relation as presented here. The second way is to synthesize the pressure–volume relationship from the force–velocity relationship as attempted by Beneken and DeWit (1967). Beneken's synthesis was based on physiological data on the instantaneous force–velocity relation which were determined by Sonnenblick (1965) by quick release afterloaded isotonic contractions of mammalian papillary muscle. The synthesized pressure–volume relationship compared favorably with physiological data. The concept of time-varying "ventricular elastance" similar to $e(t)$ was introduced as an approximation of computed pressure–volume relationships. However, it is not clearly described in Beneken's analysis how the instantaneous elastance changes by alterations in preload, afterload, contractile state and heart rate.

The present analytical approach starts from the experimentally observed curves which represent instantaneous pressure–volume ratio of the canine left ventricle. The force–velocity relations reduced via mathematical analysis are quite consistent with those directly determined on papillary muscles.

The analytical results clearly indicate that the pressure–volume ratio and the force–velocity relation are mutually transformable by employing the geometry of the ventricle. We can then estimate the force–velocity curve of myocardial contractile element by knowing the time course and magnitude of the pressure–volume ratio $e(t)$. The advantage of using $e(t)$ rather than analyzing pressure and volume variables individually is fully demonstrated by this present analysis. The effects of various interventions on the force–velocity relationship can be directly estimated by comparing the peak value and duration of a given $e(t)$ with those of a control $e(t)$, $e_o(t)$, in the same ventricle. On the other hand, the effects of preload ventricular volume and afterload arterial pressure on ventricular pressure and volume variables conveniently cancel out when one looks at the ratio of these two variables. On these basis, we conclude that $e(t)$ can be used as a useful index of ventricular contractility on the ventricular chamber level quite consistent with known myocardial fiber mechanics. We can also conclude that $e(t)$ serves as a bridge between the two levels of characterization of the heart as a pump, one on the ventricular chamber level and the other on the myocardial level.

APPENDIX I

Nine mongrel dogs (19 ~ 21 kg) were anesthetized with chloralose (60 mg/kg) and urethane (600 mg/kg) given intravenously. A midsternal thoracotomy was

performed under positive pressure ventilation. After bilateral vagotomy the stellate ganglia were removed. Total right heart bypass was initiated by draining venous return via the caval veins into a blood reservoir, from which a pump perfused the blood into the pulmonary artery. Coronary venous return to the right heart was drained into the same reservoir by negative hydrostatic pressure. By this method the right ventricle was sufficiently collapsed for our present purpose. The left intraventricular volume was measured using a plethysmographic technique. The principle of this method is to assess the volume change from the air pressure change in the air-tight chamber in which the ventricle is enclosed. We modified the classic cardiometer system (Wiggers, 1952) in order to eliminate any air leak and temperature drift. The observed pressure drift of the present cardiometer system was equivalent to less than ± 0.5 ml in 3 h. Its dynamic response was flat from 0 to 15 Hz. The sensitivity of the cardiometer system was precalibrated by changing a known volume of air within the cardiometer system. Zero intraventricular volume was calibrated at the end of experiment by withdrawing all the blood in the left ventricular lumen.

The load-independency of the instantaneous pressure–volume ratio of the left ventricle was studied while changing cardiac output ($\pm 50\%$ around 80 ml/kg/min) with and without secondary changes in mean arterial pressure. Alternately mean arterial pressure was changed ($\pm 50\%$ around 100 mmHg) without any secondary change in cardiac output. These changes in preload and afterload were performed by connecting an auxiliary pump between any pair of the blood reservoir, the left atrium and the femoral artery.

APPENDIX II

Previously Suga defined $e(t)$ as the ratio of left intraventricular pressure $p(t)$ to intraventricular absolute volume $v_i(t)$ which was estimated by indicator dilution method and aortic flow measurement (Suga, 1969a, 1969b, 1970 and 1971a). Recently left intraventricular absolute volume $v_i(t)$ was measured in canine hearts with a sensitive cardiometer in combination with a total right heart bypass. It was found that the peak $e(t)$ became more independent of ventricular loading conditions when the volume $v_i(t)$ was corrected by a small constant volume v_d $2 \sim 4$ml in a 13-kg dog (Suga *et al.*, 1971) and $4 \sim 6$ ml in a 20-kg dog (Suga *et al.*, submitted for publication). Therefore we redefined $e(t)$ in this paper as $e(t) \equiv p(t)/[v_i(t) - v_d]$.

It becomes necessary to use this correction factor, v_d, when we attempt to find a linear correlation between the endsystolic ventricular pressure and ventricular volume. This correction factor is also evident from Monroe and French's (1961) experimental data on pressure–volume loops of an excised left ventricular preparation (Fig. 10). The pressure–volume loops in Fig. 10 were determined from a ventricle contracting auxotonically against an air-filled compression chamber. Despite the alterations in preload and afterload, the endsystolic pressure–volume data points of these contractions are scattered around a single rectilinear line which was drawn by us. This line intercepts with the volume axis at a small volume (about 5 ml from these data) which corresponds to the v_d used in the calculation of $e(t)$ in our analysis. From other data in Monroe and French's paper it is

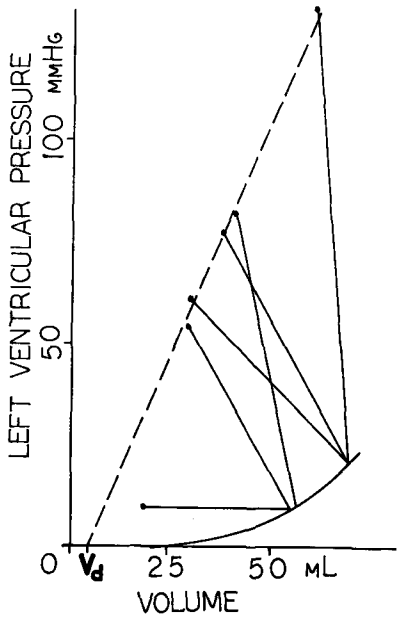

FIG. 10. Left intraventricular pressure–volume loops contracting from different end-diastolic volumes against an air-filled compression chamber with varied volume compliance [Reproduced from Fig. 12 of Monroe and French (1961) with the permission of the author and publisher]. The broken line is drawn by us so that all of the maximum pressure points will be located on or near it. v_d is the volume axis intercept of this line.

evident that if we subtract a small volume from the endsystolic volumes and then divide these corrected volumes into the concomitant endsystolic pressure, we obtain almost identical pressure–volume ratio values regardless of widely different preload and afterload conditions imposed on the ventricle.

APPENDIX III

Listed below are the mathematical forms of f_1, f_2 and their derivatives with respect to v_i, which are used in the calculation of $F(t)$ and $V_{ce}(t)$. These differ with the type of geometric model to be used.

1. Sphere Model

$$f_1(v_i) = v_i^{2/3}(v_i - v_d)/[(v_{io} + v_m)^{2/3} - v_{io}^{2/3}],$$
$$f_2(v_i) = [(v_i + v_m)^{1/3} + v_i^{1/3}]/[(v_{io} + v_m)^{1/3} + v_{io}^{1/3}],$$
$$df_1(v_i)/dv_i = [5/3 \cdot v_i^{2/3} - 2/3 \cdot v_d v_i^{-1/3}]/[(v_{io} + v_m)^{2/3} - v_{io}^{2/3}],$$
$$df_2(v_i)/dv_i = [1/3 \cdot (v_i + v_m)^{-2/3} + 1/3 \cdot v_i^{-2/3}]/[(v_{io} + v_m)^{1/3} + v_{io}^{1/3}].$$

2. Cylinder Model

$$f_1(v_i) = v_i^{1/2}(v_i - v_d)/[(v_{io} + v_m)^{1/2} - v_{io}^{1/2}],$$
$$f_2(v_i) = [(v_i + v_m)^{1/2} + v_i^{1/2}]/[(v_{io} + v_m)^{1/2} + v_{io}^{1/2}],$$
$$df_1(v_i)/dv_i = [3/2 \cdot v_i^{1/2} - 1/2 \cdot v_d v_i^{-1/2}]/[(v_{io} + v_m)^{1/2} - v_{io}^{1/2}],$$
$$df_2(v_i)/dv_i = [1/2 \cdot (v_i + v_m)^{-1/2} + 1/2 \cdot v_i^{-1/2}]/[(v_{io} + v_m)^{1/2} + v_{io}^{1/2}].$$

ACKNOWLEDGMENT

The authors gratefully acknowledge the assistance of Dr. Artin A. Shoukas in preparation of this manuscript.

REFERENCES

ARMOUR, J. A., AND RANDALL, W. C. Structural basis for cardiac function. *American Journal of Physiology* 1970, **218,** 1517–1523.

BENEKEN, J. E. W., AND DEWIT, B. A physical approach to hemodynamic aspects of the human cardiovascular system. E. B. Reeve and A. C. Guyton, (Eds.) *Physical bases of circulatory transport: Regulation and exchange.* Philadelphia, PA: W. B. Saunders, 1967, pp. 1–45.

BRAUNWALD, E., ROSS, J., JR., AND SONNENBLICK, E. H. *Mechanisms of contraction of the normal and failing heart.* Boston MA:, Little Brown and Co., 1967.

BRUTSAERT, D. L., AND SONNENBLICK, E. H. Force-velocity-length-time relations of the contractile elements in heart muscle of the cat. *Circulation Research* 1969, **24,** 137–149.

DONDERS, J. J. H., AND BENEKEN, J. E. W. Computer model of cardiac muscle mechanics. *Cardiovascular Research* 1971, Suppl. No. 1, 34–50.

DOWNING, S. E., AND SONNENBLICK, E. H. Cardiac muscle mechanics and ventricular performance: Force and time parameters. *American Journal of Physiology* 1964, **207,** 705–715.

FRANK, O. Zur Dinamir des Herzmuskels. *Zeitschrift fuer Biologie* 1895, **32,** 370–447.

FRY, D. L., GRIGGS, D. M., JR., AND GREENFIELD, J. C., JR. Myocardial mechanics; tension-velocity-length relationships of heart muscle. *Circulation Research* 1964, **14,** 73–85.

KAVALER, F., HARRIS, R. S., LEE, R. J., AND FISHER, V. J. Frequency-force behavior of in situ ventricular myocardium in the dog. *Circulation Research* 1971, **28,** 533–544.

LEVINE, H. J., AND BRITMAN, N. A. Force-velocity relations in the intact dog heart. *Journal of Clinical Investigation* 1964, **43,** 1383–1396.

MCDONALD, R. H., JR., TAYLOR, R. R., AND CINGOLANI, H. E. Measurement of myocardial developed tension and its relations to oxygen consumption. *American Journal of Physiology* 1966, **211,** 667–673.

MIRSKY, I. Left ventricular stresses in the intact human heart. *Biophysical Journal* 1969, **9,** 189–208.

MONROE, G., AND FRENCH, G. M. Left ventricular pressure-volume relationships and myocardial oxygen consumption in isolated heart. *Circulation Research* 1961, **9,** 362–374.

PARMLEY, W. W., AND SONNENBLICK, E. H. Series elasticity in heart muscle; its relation to contractile element velocity and proposed muscle models. *Circulation Research* 1966, **20,** 112–123.

PARMLEY, W. W., YEATMAN, L. A., AND SONNENBLICK, E. H. Differences between isotonic and isometric force-velocity relations in cardiac and skeletal muscle. *American Journal of Physiology* 1970, **219,** 546–550.

PARMLEY, W. W., CHUCK, L., AND SONNENBLICK, E. H. Relation of V_{max} to different models of cardiac muscle. *Circulation Research* 1972, **30,** 34–43.

PATTERSON, S. W., PIPER, H., AND STARLING, E. H. The regulation of heart beat. *Journal of Physiology* 1914, **48,** 465–513.

ROSS, J., JR., COVELL, J. W., SONNENBLICK, E. H., AND BRAUNWALD, E. Contractile state of the heart characterized by force-velocity relations in variably afterloaded and isovolumic beats. *Circulation Research* 1966, **18,** 149–163.

SAGAWA, K. Analysis of the ventricular pumping capacity as a function of input and output pressure loads. In E. B. Reeve and A. C. Guyton, (Eds.), *Physical bases of circulatory transport: Regulation and exchange.* Philadelphia, PA: W. B. Saunders, 1967, pp. 141–149.

SANDLER, H., AND DODGE. H. T., Left ventricular tension and stress in man. *Circulation Research* 1963, **13,** 91–104.

SARNOFF, S. J., AND MITCHELL, J. H. The control of the function of the heart. In *Handbook of Physiology: II. Circulation,* Vol. 1, American Physiological Society, 1962, pp. 489–532.

SONNENBLICK, E. H. Force-velocity relations in mammalian heart muscle. *American Journal of Physiol.* 1962, **202,** 931–939.

SONNENBLICK, E. H. Determinants of active state in heart muscle; force, velocity, instantaneous muscle length, time. *Federation Proceedings* 1965, **24,** 1396–1409.

SUGA, H. Analysis of left ventricular pumping by its pressure–volume coefficient. *Japanese Journal of Medical Electronics and Biological Engineering* 1969a, **7,** 406–415 (in Japanese).

SUGA, H. Time course of left ventricular pressure–volume relationship under various enddiastolic volume. *Japanese Heart Journal* 1969b, **10,** 509–515.

SUGA, H. Time course of left ventricular pressure–volume relationship under various extents of aortic occlusin. *Japanese Heart Journal* 1970 **11,** 373–378.

SUGA, H. Left ventricular time-varying pressure–volume ratio in systole as an index of myocardial inotropism. *Japanese Heart Journal* 1971a, **12,** 153–160.

SUGA, H. Theoretical analysis of a left ventricular pumping model based on the systolic time-varying pressure–volume ratio. *IEEE Transactions in Biomedical Engineering* 1971b, **18,** 47–55.

SUGA, H., KAMIYA, A., AND TOGAWA, T. Left ventricular volume measurement by cardiometry with complete right heart bypass (abstract) *Journal of Physiological Society of Japan* 1971, **33,** 451.

WIGGERS, C. J. *Circulatory dynamics.* New York: Grune and Stratton, 1952.